Survey Review, **37**, 288 (April 2003)

EXPERIMENTS WITH TWO DIFFERENT APPROACHES TO GRIDDING TERRESTRIAL GRAVITY ANOMALIES AND THEIR EFFECT ON REGIONAL GEOID COMPUTATION

J M Goos

Physical, Geometric and Space Geodesy Section,
Delft University of Technology, The Netherlands

W E Featherstone, J F Kirby, S A Holmes

Western Australian Centre for Geodesy,
Curtin University of Technology, Western Australia

ABSTRACT

This paper compares the gridding of two types of terrestrial gravity anomaly prior to the computation of regional gravimetric geoid models over Australia. The aim is to investigate the effects of high-frequency components (by way of the terrain correction) on the resulting grid of mean gravity anomalies, and hence the geoid. The gravity anomaly types investigated comprise simple Bouguer anomalies and refined Bouguer anomalies, both computed using a constant topographic mass density. Irrespective of which anomaly type is used for gridding, the relevant additional correction terms are applied to yield an approximation of the mean Helmert anomaly. Regional gravimetric geoid models are then computed over Australia and compared with one another and with GPS-levelling points on the Australian Height Datum. This shows that the application of terrain corrections before or after gravity gridding has only a relatively small effect on the computed geoid in Australia.

INTRODUCTION

The fast Fourier transform (FFT) technique for regional gravimetric geoid determination, which is normally necessary for the practical computation of a high-resolution geoid model over large areas such as Australia [**e.g., 34**], requires a regular geographic grid of mean gravity anomalies [**e.g., 30**]. However, quadrature-based numerical integration can also require a regular geographic grid or concentric circular compartments of mean gravity anomalies [**e.g., 17, 25**]. In order to predict gravity anomalies in these regular configurations from irregularly spaced gravity observations, interpolation - and sometimes extrapolation - is required.

As is well known from signal sampling theory [**2, 3**], these gridding processes are subject to a phenomenon called aliasing in the presence of improperly sampled high frequencies. That is, if there are insufficient observations to sample the complete gravity field spectrum, then high-frequency signals are incorrectly propagated (i.e., aliased) into the low frequencies. This generates spurious long-wavelength terrestrial gravity anomalies that will contaminate the computed geoid, especially if unmodified Stokes's kernels are used over large areas [**36**].

Simple Bouguer gravity anomalies were gridded during the production of the most recent gravimetric geoid model of Australia, termed AUSGeoid98 [**12**]. The reason for not using refined Bouguer gravity anomalies (i.e., simple Bouguer anomalies plus gravimetric terrain correction) was that they do not allow the subsequent computation of accurate mean Faye gravity anomalies in each geographic grid element [**8**]. However, the simple Bouguer correction omits the high-frequency effects of the terrain residual to the Bouguer plate, and is thus subject to aliasing *if the gravity observation sampling is inadequate*. [**12**], while acknowledging this potential limitation, argue that it is probably more important to use the full resolution of the digital elevation model by applying the mean terrain correction at a later stage.

This paper presents the results of experiments to compare the use of simple and refined Bouguer gravity anomalies for data prediction onto a regular geographic grid, and the effect that this has on the geoid computed using the unmodified Stokes kernel with no truncated spherical cap via the one-dimensional fast Fourier transform (1D-FFT) technique [**16**]. This is to resolve the doubt over whether simple Bouguer anomalies are acceptable for gravity data gridding in the Australian context. Importantly, whichever technique is selected, the components of the gravity field spectrum that are removed are subsequently restored to yield mean Faye gravity anomalies, as an approximation of mean Helmert gravity anomalies.

The Effects of Aliasing and Unrepresentative Sampling on Gravimetric Geoid Computation

Aliasing is the false translation of any signal's power from the high frequencies into the low frequencies due to undersampling [**2, 3**]. This causes any high frequencies present in the sampled signal to be underestimated, while the low frequencies present in that signal are overestimated. Specifically, the high frequencies are *aliased* into the low frequencies. Therefore, any undersampling of a signal can cause aliasing. However, the term aliasing, as used in the digital signal processing literature, generally refers to *regular* undersampling of a signal, which is rarely the case with gravity observations. As such, a distinction needs to be made here.

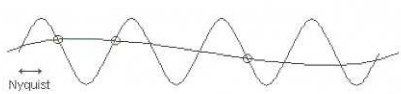

Fig. 1. A schematic of 'aliasing' due to unrepresentative sampling: the sinusoidal line is the desired signal, the circles are the irregular sample points; subsequent interpolation of the sample points gives a low-frequency artefact that is not present in the sampled sinusoidal signal.

A more accurate terminology applied to observations of the Earth's gravity field is *aliasing due to unrepresentative sampling* (herein termed pseudo-aliasing), because gravity is rarely sampled in any regular configuration (cf. Figure 2). Nevertheless, unrepresentative sampling will also generate the same effect as classical aliasing, as illustrated schematically in Figure 1. This is especially the case when the distances between some samples are greater than one-half of the wavelength of whole the signal to be sampled (cf. the Nyquist frequency in classical aliasing).

In gravimetric geoid computation, this *pseudo-aliasing* occurs if there are insufficient gravity observations available to sample the entire gravity field spectrum. This is governed by the practicalities of gravity data acquisition in the field. For instance, many gravity observations are made along roads or tracks through areas of rugged terrain, and because these often follow the valleys, these observations are made systematically too low [**e.g., 8**].

In Australia, an opposite effect occurs in flatter regions, where observations were made using helicopters for transport [**27**]. These observations were often made on higher parts of the terrain where convenient landing spots were found, and thus these observations are made systematically too high. In addition, there is unrepresentative sampling of the entire gravity field spectrum in areas where very few or no gravity observations are made, simply because field access is too difficult.

The problem of pseudo-aliasing due to unrepresentative sampling of gravity data will degrade the computed geoid, which can be prevented by either (1) reducing the gravity observation spacing; or (2) removing the high frequencies present in the sampled signal using another data source before interpolation, and then restoring them afterwards.

Option (1) above is rarely practical, since denser sampling of the gravity field signal can only be achieved by using more observations, which simply have not been made. Therefore, without collecting additional gravity data (which is often impractical or too costly), alternative strategies must be adopted to reconstruct the best possible gravity anomaly signal for subsequent geoid computation.

Option (2) above involves using supplementary information about the high-frequency content of the gravity anomaly signal in a remove-grid-restore procedure. If such information is available, this provides the preferable approach. Here, additional high-frequency gravity field information is provided by terrain corrections, which are based on a digital elevation model that has a denser (and usually regular) sampling interval than the gravity observations. Of course, other artificial constructs could be employed, but these would have no physical meaning and hence their use would be questionable. Since density information is not yet available for the entire Australian continent, this study will only use simple and refined Bouguer gravity anomalies based on a constant topographic mass-density.

Finally, the problem of aliasing and pseudo-aliasing due to unrepresentative sampling of the Earth's gravity field spectrum is not new, and has been studied by many authors, albeit in slightly different contexts to this study [**e.g., 37, 31, 21**].

THE AUSTRALIAN GRAVITY FIELD DATA

Terrestrial gravity data

The terrestrial gravity data used for these experiments are taken from the 2001 release of Geoscience Australia's (formerly the Australian Geological Survey Organisation, AGSO) national gravity database [**27**]. This database comprises over 700,000 gravity observations on land only (see later), after removal of suspect surveys already identified by Geoscience Australia. The observation spacing of these data is at least ~11 km (~7 km in South Australia), with increased resolution in areas of resource exploration or other interest (Figure 2). Moreover, the gravity data coverage is largely complete in Australia, with no large data gaps. Accordingly, the pseudo-aliasing effects of unrepresentative sampling are probably less in Australia than in other regions that have a poorer gravity data coverage.

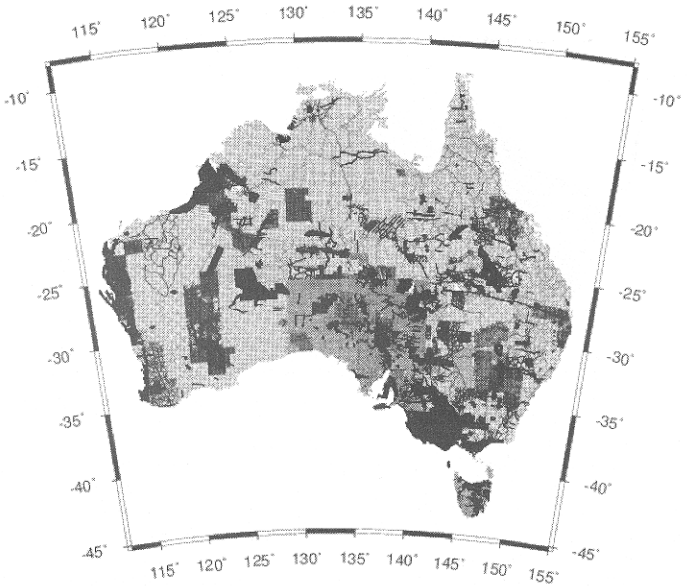

Fig. 2. Spatial coverage of gravity observations in the 2001 data release from Geoscience Australia

Topographic elevation data

The digital elevation model (DEM) used in this study is the version 2 GEODATA 9 arc-second DEM of Australia [**18**]. This supersedes the version 1 model [**4**], which was found to contain gross errors (i.e., horizontal gradients of up to 76 degrees) that adversely affect the computation of gravimetric terrain corrections [**23, 24**]. Incorrect flow directions of the stream data used to constrain the version 1 DEM caused these spurious gradients (Hutchinson, 2000 pers. comm.), which have now been removed. This allows the full 9 arc-second resolution of the version 2 DEM to be used to compute Moritzian gravimetric terrain corrections (Figure 3 and [**10**])

Table 1 shows descriptive statistics of the version 1 and version 2 GEODATA 9 arc-second DEM grids and the corresponding terrain corrections: the 27 arc-second grid from [**23**]; and the 9 arc-second grid from [**10**]. The 27 arc-second grid of terrain corrections from the version 1 DEM was used to compute AUSGeoid98 [**12**]. However, only the 9 arc-second terrain corrections from the version 2 DEM will be used in this study

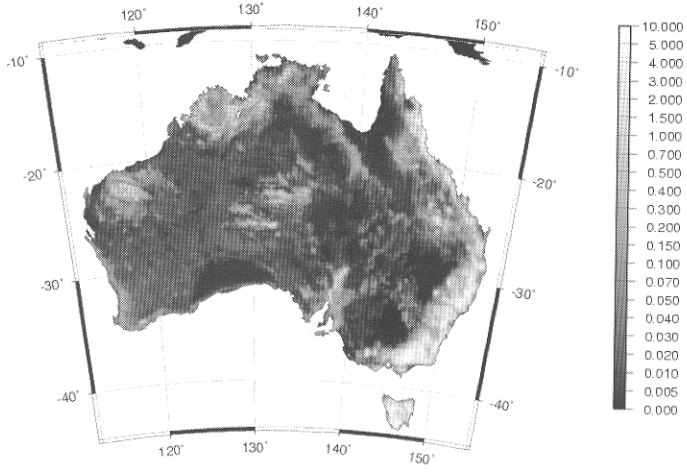

Fig.3. Generalised image of the 9 arc-second gravimetric terrain corrections on land computed from the version 2 GEODATA 9 arc-second DEM of Australia (Units in mGal. Mercator projection)

Importantly, the version 2 grid of terrain corrections [**10**] provides higher frequency terrain corrections to Australian gravity observations than previously available. However, the Australian terrain corrections (Table 1) are smaller than those encountered in other countries with larger topographic relief, as expected. Therefore, the contribution of these corrections to the Australian geoid (and their contribution to reducing pseudo-aliasing) is expected to be relatively small.

Table 1. *Descriptive statistics of the Australian digital elevation models (DEMs) and corresponding Moritzian gravimetric terrain corrections (TCs)*

	Max	*Min*	*Mean*	*STD*
Version 1, 9 arc-second DEM (metres)	2193.4	-23.8	133.6	190.2
[erroneous] 9 arc-second TCs (mGal)	273.6	0.0	0.8	0.5
27 arc-second TCs (mGal)	40.2	0.0	0.1	0.4
Version 2, 9 arc-second DEM (metres)	2228.0	-16.0	272.0	191.5
9 arc-second TCs (mGal)	86.9	0.0	0.2	0.7

Since 2001, Geoscience Australia has largely dispensed with the ship-track data in its national gravity database. The primary reasons for this appear to be the superior marine gravity data coverage now offered by satellite radar altimetry, and that the ship-track gravity data are not provided in a format so as to allow crossover corrections to be applied. Figure 4 shows the differences between the GMGA97 multi-mission altimeter database [**20**] and the ship-track gravity observations from the 1998 AGSO gravity data release. This shows that large (>10 mGal) differences exist between adjoining and crossing ship-tracks, thus illustrating the omission of crossover corrections from most of the 1998 AGSO ship-track data.

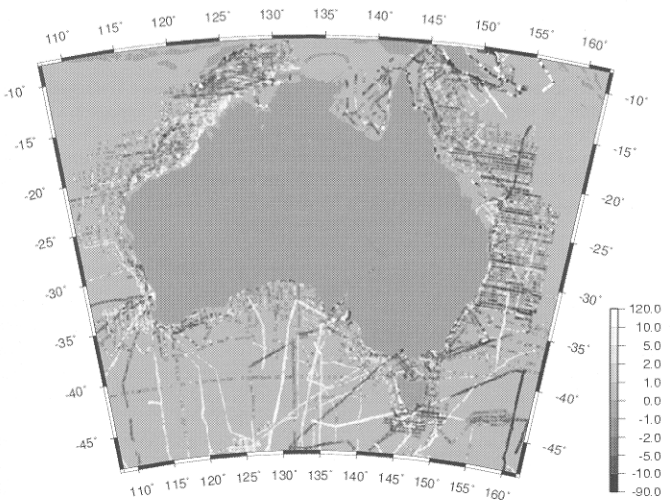

Fig.4. Differences between GMGA97 multi-mission altimeter-derived free-air gravity anomalies and the 1998 AGSO ship-track free-air gravity anomalies (units in mGal; Lambert projection)

[**7**] shows that there are significant differences among the satellite altimeter-derived gravity anomalies computed by different groups [**1, 20, 29**], especially close to the coast of Australia. This is due to the problems with correctly tracking radar returns from the coastal zone [**5**], poorly modelled shallow-sea tides, and the Gibbs phenomenon at the coasts in the FFT techniques used. Since the ship-track gravity data around Australia are generally of poor quality (described above), it is difficult to select the more precise altimeter data source. Therefore, the GMGA97 data are selected for this study purely because they appear (to the authors) to use a geodetically more rigorous theoretical basis than the approximations used by other groups [**19**].

Importantly however, the choice of the altimeter-derived gravity anomalies is not critical to this study because the same altimeter data will be used for each geoid model,

thus any errors will be common and cancel on differencing. The need to include altimeter data is to reduce the effect on the computed geoid arising from having no reliable marine gravity data offshore Australia. For instance, the omission of gravity data offshore Australia may cause low frequency artefacts in the computed geoid that will mask the effects of aliasing due to the gravity anomaly types used for gridding.

GPS-levelling data

The gravimetric geoid models computed will be compared with discrete geometrical geoid control provided by co-located GPS and spirit-levelling data, since these are the only [partly] independent data with which to verify gravimetric geoid models on land. The GPS-levelling data used are the same 1013 points as used by [**9**]. However, such comparisons are equivocal because of the errors in these data. It is now acknowledged that the GPS data used in this database comes from a variety of ages [**22**] and are thus sensitive to the quality and processing algorithms available at the time of collection. However, information is not currently available with which to identify the older, and presumably less precise, GPS data. Therefore, all 1013 points will be used in the analyses.

The spirit-levelled heights are on the Australian Height Datum (AHD; [**28**]). This vertical datum is widely acknowledged to contain distortions of approximately 1.5m from a single equipotential surface of the Earth's gravity field [**e.g., 6**]. This is due to a combination of the quality of the (predominantly third-order) spirit levelling observations used, the use of a normal orthometric height system, and the fixing of 32 tide gauges to mean sea level measured over a ~3 year period at coastal tide gauges.

CONCEPTS AND METHODS

As stated, two different types of gravity anomaly are gridded in this study: the simple Bouguer anomaly, and the refined Bouguer anomaly. The latter includes the terrain corrections described earlier. Importantly, these types of gravity anomaly are used *only* in the gridding stage. All other corrections required to compute mean Faye gravity anomalies (as an approximation of mean Helmert gravity anomalies) are applied at subsequent stages in the computation, as will be described next.

In order to reduce any pseudo-aliasing using a remove-grid-restore procedure, the high-frequency components of the gravity anomaly signal to be interpolated must be removed leaving only a smooth signal, since the amplitude and frequency of the pseudo-aliasing are determined by the smoothness of the anomaly used for gridding. This will be tested using only the terrain correction (other contributing factors will be described later). Importantly, the high-frequency signals that are removed before gridding must subsequently be restored in order to preserve both the mass of the Earth and the information content of the gravity anomaly signal obtained after gridding.

The many different gridding algorithms available (e.g., polynomials, splines, Kriging, collocation) will not be explicitly tested in this study. Instead, the tensioned spline algorithm [**33**] will be used, primarily because this is readily available in the GMT (Generic Mapping Tools) software [**38**] and is suited to gridding potential field data. A bi-cubic spline will also be used (described later). As such, this study concentrates on the suitability of the two different types gravity anomaly, rather than the gridding algorithm, which forms an entirely different scope of study [**39**].

Figure 5 shows a schematic diagram of the concepts involved in gridding gravity data for this study. In what follows, the peculiarities of the Australian data will be explained within this general framework.

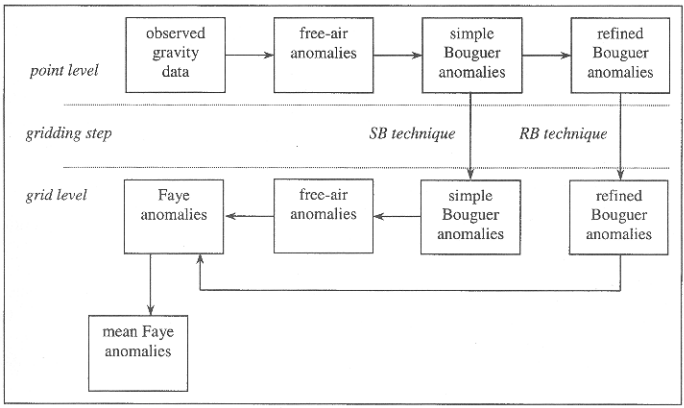

Fig.5. Flowchart of the two different techniques tested to compute a regular grid of mean Faye gravity anomalies prior to gravimetric geoid computation

Gridding with simple Bouguer gravity anomalies in Australia

As stated, simple Bouguer anomalies were used in the production of AUSGeoid98 [**12**]. The simple Bouguer plate reduction may account for a large amount of the terrain effect on observed gravity, and can remove *some* of the high-frequency content of the gravity signal (especially when compared to the free-air gravity anomaly). Theoretically, simple Bouguer anomalies are less prone to aliasing than free-air anomalies, but are more so than refined Bouguer anomalies.

The use of simple Bouguer anomalies in this study, herein termed the *SB technique*, consists of four stages (adapted from [**8**]). Of course, other adaptations of this technique may have to be applied in other regions.

- Stage SB1: Compute simple Bouguer gravity anomalies at the gravity observation points on land using normal gravity on the reference ellipsoid computed from Somigliana's formula, the second-order free-air gravity reduction, the atmospheric gravity correction, and the simple plate Bouguer correction based on a constant topographic mass density of 2670 $kg.m^{-3}$ [**e.g., 11**]. The approximation of a constant topographic mass density has to be used because no Australia-wide density model is currently available (see later discussion). The elevations used to compute these gravity anomalies are those supplied in the Geoscience Australia database, and the horizontal positions of the gravity observations used to map the data and compute normal gravity are given on the Geocentric Datum of Australia.
- Stage SB2: Interpolate the simple Bouguer anomalies in stage SB1 from the observation points to the same nodes as the regular 2 arc-minute grid (on the

Geocentric Datum of Australia) as used for AUSGeoid98. This interpolation step used the tensioned spline algorithm [**33**].

- Stage SB3: Reconstruct free-air gravity anomalies at the 9 arc-second grid nodes by applying the reverse (i.e., add rather than subtract $2\pi G\rho H$) Bouguer plate reduction to the simple Bouguer gravity anomalies using the mean topographic height estimated by the individual DEM cell at each 9 arc-second grid point. [To achieve this in practice, a bi-cubic spline was used to interpolate from the 16 nearest 2 arc-minute grid cells of simple Bouguer anomalies to the 9 arc-second DEM grid. This was necessary in practice because GMT fails when dealing with such a high-resolution grid over Australia.] This yields a 9 arc-second grid of mean free-air gravity anomalies.

- Stage SB4: Compute mean Faye (i.e., terrain corrected free-air) gravity anomalies by area-weighted averaging (i.e., proportioned according to the overlaps between the two grids) the 9 arc-second grids of the reconstructed free-air gravity anomalies (Stage SB3) and the terrain corrections (described earlier) onto a 2 arc-minute grid. The secondary indirect effect is applied at this stage, and the GMGA97 satellite altimeter-derived gravity anomalies are also added in marine areas. The marine areas were defined by the high-resolution shoreline data contained within the GMT software [**38**].

The above four stages are essentially the same as proposed by [**8**]. Although *ibid.* acknowledge that the addition of the terrain correction to simple Bouguer anomalies would theoretically produce an even smoother surface for gridding; they instead used only the simple Bouguer anomaly so as to allow for the addition of the *mean* terrain correction to yield the mean Faye gravity anomaly in each grid cell (Stage SB4). The terrain correction was not applied to point gravity observations prior to gridding (Stage SB1) because the mean of terrain corrections *applied to point observations* is not necessarily representative of the integral mean value over the whole 2 arc-minute compartment if the gravity observation spacing is unrepresentative.

Instead, the mean terrain correction is calculated from all 9 arc second cells in each 2 arc-minute grid compartment from Stage SB4 because this is expected to be a more accurate representation of the integral mean value over the whole compartment. This is because it is computed from regularly distributed data points, using all of the computed 9 arc-second terrain corrections, instead of being applied to only irregularly spaced point observations. [**8**] argue that by including terrain information from areas not sampled by a gravity meter through applying the terrain correction after gridding, both the spatial resolution and accuracy of the computed grid of mean Faye gravity anomalies can be increased.

Another perceived advantage of the above approach is that an additional gridding stage is avoided. Specifically, the terrain corrections computed from a DEM are also given on a regular 9 arc-second grid. Therefore, to obtain the terrain corrections at the irregularly spaced gravity observation points, the values of the gridded terrain corrections near the irregular observation point must first be interpolated to each observation point. This may generate an additional interpolation error, especially if the DEM and hence terrain corrections are not of a sufficiently high resolution so as to avoid aliasing. In addition, the mean heights in each element of the DEM are not necessarily equal to the height of the gravity observations. Averaging the terrain corrections (Stage SB4) does not require any interpolation, and is therefore assumed to be insensitive to any such aliasing.

Gridding with refined Bouguer gravity anomalies in Australia

Since refined Bouguer anomalies are theoretically smoother than simple Bouguer anomalies, they are expected to be less sensitive to pseudo-aliasing and are therefore assumed to be more suitable for gridding. With simple Bouguer anomalies, only a Bouguer plate reduction has been applied, and a high-frequency gravity signal (from the terrain correction) will still be present in the anomalies, thus causing some degree of pseudo-aliasing to occur if there is unrepresentative sampling of the gravity field spectrum by the gravity observations used.

However, applying the Australian terrain corrections before gridding will not necessarily remove all of the high frequencies omitted by the Bouguer plate reduction, since the terrain correction is computed as a bandwidth limited signal that omits near-meter effects [**23, 10**]. This being said, applying the terrain corrections should remove a large part of the high frequencies that are omitted by the simple Bouguer correction. As will be discussed below, to obtain Faye anomalies out of these refined Bouguer anomalies, only a reverse Bouguer plate reduction needs to be performed.

The use of refined Bouguer anomalies for the data gridding in this study (herein termed the *RB technique*) consists of the following five stages. Again, other adaptations of this technique may have to be applied in other regions.

- Stage RB1: Compute simple Bouguer gravity anomalies from the land gravity observation points using exactly the same approach as used for Stage SB1.
- Stage RB2: Interpolate the terrain corrections to the gravity observation points from the nodes of the regular 9 arc-second grid of previously computed terrain corrections. Bi-cubic spline interpolation, as opposed to the tensioned spline in GMT, was used in this study purely because of data management issues. [The 9 arc-second grid of terrain corrections over Australia occupies nearly 1 Gb of computer disc space, even when stored in binary format. If converted to the format required by GMT, then the resulting grid would be too cumbersome to deal with, as well as the memory allocation in GMT failing.] These interpolated terrain corrections (see Remark 1 below) are added to the point simple Bouguer gravity anomalies to yield point refined Bouguer gravity anomalies.
- Stage RB3: Interpolate the refined Bouguer anomalies from the observation points to the same nodes as the regular 2 arc-minute grid (on the Geocentric Datum of Australia) as used for AUSGeoid98. This uses the tensioned spline algorithm [**33**], so as to be consistent with the gridding of the simple Bouguer anomalies in Stage SB3.
- Stage RB4: Reconstruct Faye gravity anomalies at the 9 arc-second grid nodes by applying the reverse Bouguer plate reduction to the interpolated (using the bi-cubic spline; see stage SB3) *refined* Bouguer gravity anomalies, based on the mean height of the DEM cell at each grid point. This yields a 9 arc-second grid of mean Faye gravity anomalies. These are directly Faye anomalies because the free-air correction and terrain correction are preserved after application of the reverse Bouguer correction. However, see Remark 2 below.
- Stage RB5: Area-weighted average the 9 arc-second grid of reconstructed Faye gravity anomalies onto the same 2 arc-minute grid as used for AUSGeoid98. As for Stage SB4, the secondary indirect effect is applied, and the GMGA97 altimeter-derived gravity anomalies are added in marine areas.

Remark 1:
If the DEM is not of a sufficiently high resolution to sample the high frequencies in the gravity field spectrum (e.g., due to near-gravimeter terrain effects in areas of rugged terrain), aliasing will occur in this interpolation stage, thus somewhat negating the aim of using refined Bouguer anomalies. Therefore, even though the refined Bouguer anomaly is theoretically smoother than the simple Bouguer anomaly, aliasing during the interpolation of terrain corrections from a precomputed grid must be taken into consideration, especially for low-resolution DEM grids. Of course, this effect will not occur if terrain corrections are computed directly at each observation point (e.g., using Hammer charts). However, the cumbersome nature of computing Hammer terrain corrections mean that they have not been computed in this way for the Australian gravity data, with the exception of some rugged parts of Tasmania [**27**].

Remark 2:
There is a disparity between the mean of the interpolated terrain corrections applied to the point gravity observations contained in a compartment (RB technique) versus the mean of the terrain corrections from all DEM elements within that compartment (SB technique; [**8**]). Therefore, the mean value of the Faye gravity anomaly in the RB technique will generally be different (and less accurate as argued by [**8**]) to that in the SB technique.

Take the following instructive example of a single point gravity observation made in a lowland part of a compartment that contains mountains on which gravity observations have not been made. The terrain correction to this point gravity observation will be small because the terrain correction decreases as a function of increasing distance from the gravitating masses (as long as no steep mountains are close to the gravity observation). Therefore, the mean terrain correction for this grid element (as per the RB technique) will not necessarily be representative of the integral mean value over the whole compartment. Conversely, the SB technique (though potentially more subject to pseudo-aliasing) uses the mean of all terrain corrections in this larger compartment, thus giving a more accurate estimate of the integral mean value.

In summary, the differences in geoid solutions resulting from the SB gridding technique versus the RB gridding technique are a consequence of the following considerations:

- Gridding refined Bouguer anomalies should produce less pseudo-aliasing than gridding simple Bouguer anomalies due to the theoretical difference in smoothness of these types of anomaly.
- Gridding refined Bouguer anomalies may produce an additional aliasing error coming from the need to interpolate the terrain correction to point gravity observations from a precomputed grid of terrain corrections (which applies in Australia).
- If terrain corrections are applied to irregularly spaced point observations before gridding refined Bouguer anomalies, this may produce an error in the computed mean if the gravity observations are unrepresentative samples of the whole gravity field spectrum in each compartment.

The role of topographic density data

All of the previous discussions have assumed that the terrain correction is the sole way to smooth the Earth's gravity field prior to gravity anomaly gridding. However, there are other equally (or more) important physical phenomena that affect the smoothness of the Earth's gravity field [**e.g., 39**].

A very important, though often neglected, consideration in the computation of both simple and refined Bouguer gravity anomalies for gridding prior to geoid computation is the unrealistic assumption of a constant topographic mass density of 2,670 $kg.m^{-3}$. This approximation is often unrepresentative of the actual mass density distribution in the topography, where large horizontal spatial variations in mass density of over 600 $kg.m^{-3}$ can occur [**17, 35**]. Since these density variations are not accounted for by a DEM when assuming a constant topographic mass density, this effect cannot be modelled by the terrain correction and thus too can cause aliasing.

In many areas of Australia, the topography is relatively smooth, whereas there are large changes in observed gravity over short distances. The relatively smooth topography of the Australian continent is due to its geological age, where different rock types have been weathered down to the same elevation. Accordingly, the terrain corrections are relatively small over most of Australia (Figure 2 and Table 1). However, large lateral changes in gravity can exist in these heavily weathered regions due to juxtaposing geological structures of different mass-density [**35**]. Therefore, high-frequency spatial variation in the Earth's gravity field will occur such that any application of the simple Bouguer correction or terrain correction (which will be small in areas of smooth topography) based on a constant topographic mass density will not reduce aliasing if the gravity field has been unrepresentatively sampled.

An instructive example comes from the Bouguer correction applied to a planar topography in which there are two different juxtaposing topographic mass densities (Figure 6). The mean elevation of the topographically flat parts of Western Australia is used for this example, which is approximately 300 m. First, the simple plate Bouguer correction for an elevation of 300 m based on a constant topographic mass density of 2,670 $kg.m^{-3}$ will yield a constant value of -33.57 mGal. Since the topography is flat, the terrain correction will be exactly zero. Therefore, the simple and refined Bouguer gravity corrections for this simple example will be equal.

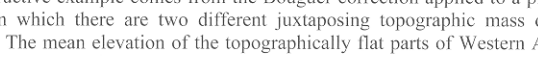

Fig.6. A flat topography of elevation 300m beneath which there are two juxtaposing geological structures of different mass density.

In the more realistic model of the topography that includes lateral variations in topographic density, the plate Bouguer corrections for the left- and right-hand sides of Figure 6 will be -28.9 mGal and –36.5 mGal, respectively. Again, the terrain correction will be close to zero because this component is dominated by changes in elevation. The change in (both simple and refined) Bouguer corrections across the simulated geological structure in Figure 6 will therefore be approximately 7.5 mGal. If the gravity field is unrepresentatively sampled across the density boundary, then pseudo-aliasing will result.

Since no nation-wide digital density model is currently available for Australia, there is an amount of pseudo-aliasing implicit to any gravity data gridding based on

both simple and refined Bouguer gravity anomalies that use a constant topographic mass density. This is one very plausible explanation for the results presented later.

RESULTS AND DISCUSSION

Gravity anomaly differences

First, it is informative to view the descriptive statistics of the 2 arc-minute grids of mean Faye gravity anomalies over the Australian landmass, which have been gridded using the SB and RB techniques, as well as their differences. Table 2 and Figure 7 show that the difference between the gravity anomaly grids is relatively small, which *indicates* that the use of the RB technique has only removed a small proportion of any pseudo-aliasing in relation to the SB technique. Recall that both are based on a constant topographic density of 2,670 kg.m^{-3}, and the Australian gravity data coverage is reasonably complete (Figure 2)

Table 2. *Statistics of the 2 arc-minute grids of mean Faye gravity anomalies on land resulting from the SB and RB gravity gridding techniques, as well as their differences (units in mGal)*

	Max	*Min*	*Mean*	*STD*
Mean Faye from the SB technique	171.029	-112.734	3.814	±24.375
Mean Faye from the RB technique	166.821	-112.704	3.792	±24.341
Residual Faye from the SB technique	107.349	-271.291	-2.290	±18.973
Residual Faye from the RB technique	103.141	-271.291	-2.313	±18.956
Difference between mean Faye (SB) and mean Faye (RB)	17.227	-12.128	0.023	±0.320

The descriptive statistics in Table 2 and the mapped differences in Figure 7 do not clearly indicate any low-frequency content of these differences. Therefore, two low-pass cosine filters (50 km and 500 km) are applied to the differences in Figure 7 to accentuate any low-frequency differences (Figures 8 and 9). The filters used are taken from the standard library of filters supplied in the GMT software [**38**]. Of course, other filters could be chosen, but the cosine filter is considered to be adequate to accentuate the low-frequency differences for this study.

From Figures 8 and 9, there is a proportion of pseudo-aliasing present in the differences. However, the amount of pseudo-aliasing is quite small. Using the ranges (i.e., maximum minus minimum) of the data used to plot Figures 7 through 9, those wavelengths greater than 50 km account for ~24% of the differences between the mean Faye gravity anomalies, and those wavelengths greater than 500 km account for ~2% of these differences. However as stated earlier, the long wavelengths in the terrestrial gravity anomalies, even if small in magnitude, have a greater effect on the computed geoid [**36**], which will be demonstrated later.

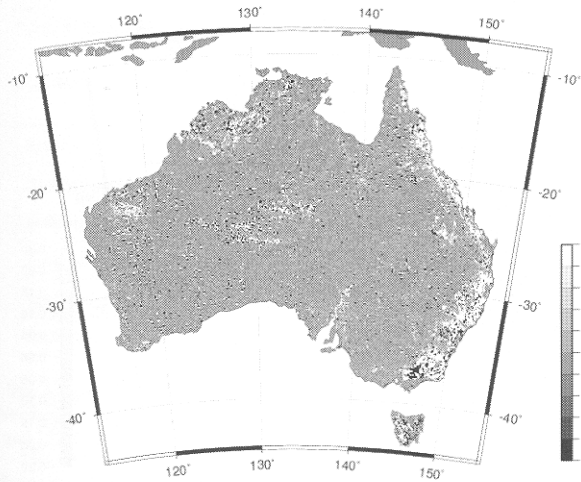

Fig.7. Differences between mean Faye gravity anomaly grids computed using the SB and RB techniques over Australia (units in mGal; Lambert projection).

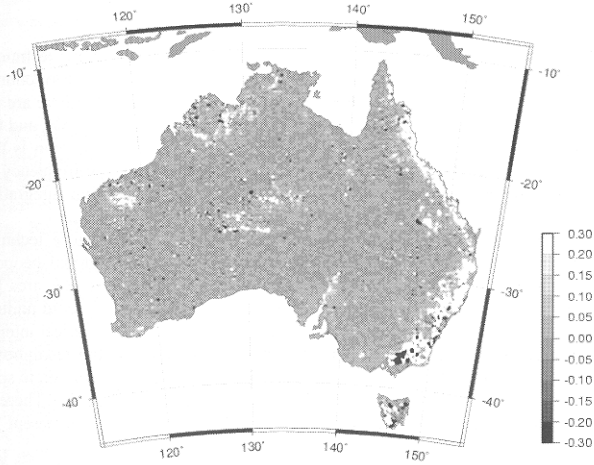

Fig.8. Medium-wavelength differences between mean Faye gravity anomaly grids computed using the SB and RB techniques from a 50 km cosine low-pass filter (units in mGal; Lambert projection).

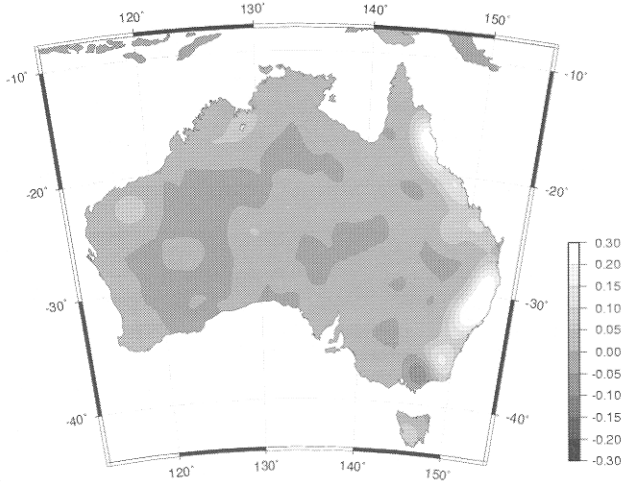

Fig.9. Long-wavelength differences between mean Faye gravity anomaly grids computed using the SB and RB techniques from a 500 km cosine low-pass filter (units in mGal; Lambert projection).

Regional geoid differences

Next, it is informative to quantify the effect of the SB and RB gridding techniques on the computed gravimetric geoid. As stated, all necessary additional correction terms have been applied to yield mean Faye gravity anomalies. Of course, there are several mathematical models with which to compute a regional gravimetric geoid, and there is currently no clear consensus on which is best. However, what is known is that the spherical Stokes kernel allows the un-attenuated propagation of low-frequency terrestrial gravity data errors into the geoid solution, especially for a larger integration domain [**36**].

Therefore, the common application of the remove-compute-restore technique is used, which is based on the complete expansion of the EGM96 global geopotential model [**26**] and an unmodified Stokes kernel applied over the entire data area [**cf. 32, 15**]. The 1D-FFT technique [**16**] was used to compute the residual geoid undulations because of its efficiency in relation to classical quadrature-based numerical integration, especially over an area the size of Australia at a 2 arc-minute spatial resolution. The above implementation of the remove-compute-restore technique is deliberate so that it is most sensitive to low-frequency errors in the terrestrial gravity data. Therefore, it will show the largest effects due to any pseudo-aliasing in the two different gravity data gridding techniques.

Table 3 shows the descriptive statistics of the two Australian geoid models computed from the two gravity data grids and their differences (cf. Figure 10). The large negative values of the residual geoid heights are due to a combination of the steep gravity gradients in the Indonesian Archipelago and the lack of terrestrial gravity data from Indonesia and Papua New Guinea to the north of Australia.

Table 3. *Statistics of the geoid heights computed via data from the SB and RB gravity gridding techniques over Australia (units in metres)*

	Max	*Min*	*Mean*	*STD*
Residual geoid via the SB technique	1.894	-20.713	-1.034	±1.639
Residual geoid via the RB technique	1.857	-20.729	-1.034	±1.640
EGM96 geoid to degree 360	85.552	-41.399	9.388	±33.291
Total geoid via the SB technique	72.792	-41.333	8.352	±32.240
Total geoid via the RB technique	72.777	-41.339	8.322	±32.233
Difference	0.147	-0.074	0.020	±0.014

The long-wavelength differences in Figure 10 are more evident than in Figure 7. Nevertheless, the 50 km and 500 km cosine filters have been applied to yield Figures 11 and 12. Again, using the ranges, the geoid wavelengths greater than 50 km account for ~75% of the differences, and those greater than 500 km account for ~43% of the differences. Comparing these to the percentages calculated for the mean Faye gravity anomalies clearly shows that the longer wavelength differences in the terrestrial gravity anomalies have a larger impact on the computed geoid differences.

This is entirely as expected because the geoid contains more power in the low frequencies than the gravity anomalies. This is exemplified by their spectral relationship (for the whole sphere) given by [**17**]

$$N_n = \frac{R}{\gamma(n-1)} \Delta g_n \qquad (1)$$

where N_n is the n-th degree surface spherical harmonic of the geoid height, R is the mean Earth radius, γ is normal gravity on the surface of the reference ellipsoid, Δg_n is the n-th degree surface spherical harmonic of the gravity anomaly.

However, the differences in Figure 10 cannot be solely attributed to pseudo-aliasing. Recall that the SB technique also uses mean terrain corrections in each 2' by 2' grid element, whereas the RB technique just uses the mean of the terrain corrections applied to the point gravity observations. Using the arguments of [**8**], the mean terrain corrections as used in the SB technique are more accurate, which explains the larger differences in mountainous areas (Figures 10 through 12), notably the Hamersley Range in northern Western Australia (centred at ~23°S, ~118°E); the Kimberley (centred at ~15°S, ~127°E); the MacDonnell Ranges in central Australia (centred at ~25°S, ~132°E); the Flinders Range near Adelaide (centred at ~33°S, ~139°E); all of the Great Dividing Range along the eastern seaboard; and Tasmania.

The feature near Melbourne (centred at ~37°S, ~146°E) is attributed to a combination of the gravity data coverage in this area, with many being made at generally higher elevations, coupled with the large terrain corrections in this region.

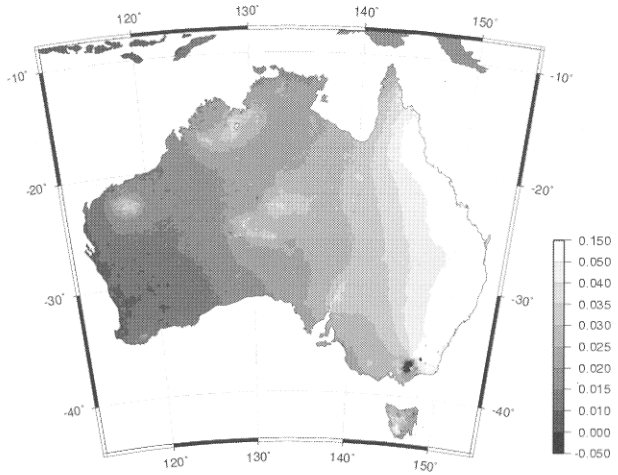

Fig.10. Differences between geoid grids computed via the SB and RB techniques (units in metres).

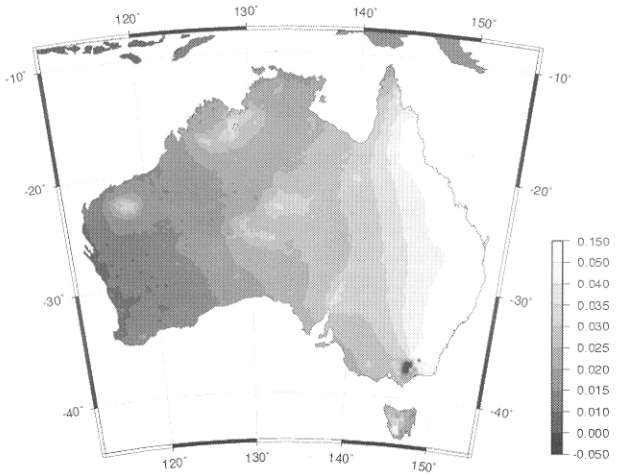

Fig.11. Medium-wavelength differences between geoid grids computed using the SB and RB techniques from a 50 km cosine low-pass filter (units in metres).

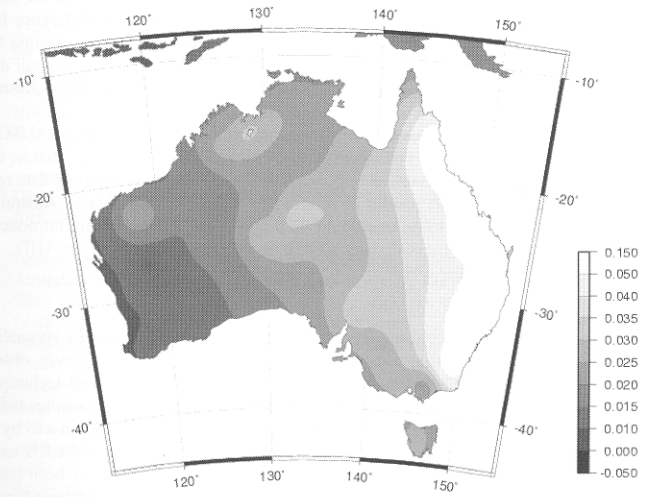

Fig.12. Long-wavelength differences between geoid grids computed using the SB and RB techniques from a 500 km cosine low-pass filter (units in metres).

Comparisons with GPS-levelling data

From the descriptive statistics and low-pass filtered gravity and geoid differences presented above, it is impossible to determine which gravity gridding technique leads to the more precise regional geoid model. Therefore, Table 4 shows the statistics of the absolute differences between the various geoid models and the 1013 GPS-levelling data. AUSGeoid98 [**12**], which was computed using a deterministically modified Stokes kernel for a one-degree cap radius, is shown by way of comparison, as is EGM96 to degree and order 360 (Table 4).

Table 4. *Statistics of the differences between the 1013 GPS-AHD data and various geoid models over Australia (units in metres)*

Geoid Model	*Max*	*Min*	*Mean*	*STD*
AUSGeoid98 (i.e., with SB technique)	3.558	-2.572	-0.002	±0.314
EGM96 geoid to degree 360	3.537	-2.441	-0.015	±0.441
Total geoid via the SB technique	5.169	-1.691	1.449	±0.741
Total geoid via the RB technique	5.222	-1.657	1.487	±0.749

The large mean difference for the two new geoid models and AUSGeoid98 in Table 4 is due to a combination of the treatment of the zero-degree term in AUSGeoid98 [**12**] and the lack of terrestrial gravity data to the north of Australia, which propagate

into the whole geoid model when not using a spherical cap. Therefore, from the standard deviations of the differences in Table 4, there is an insignificant difference between the geoid models computed via the SB and RB techniques when accounting for the errors in the GPS-levelling data used. This coupled with the reasonably small differences in Figure 10 show that the role of terrain corrections in smoothing the Australian gravity field as a means to reduce pseudo-aliasing is insignificant.

The larger standard deviations of the two new geoid models compared to AUSGeoid98 and EGM96 (Table 4) are consistent with the results of [**12, 13, 14**]. That is, the use of a limited integration domain, as opposed to the use of the entire gravity data rectangle, yields improved geoid results in relation to GPS-levelling data in Australia. Though not proven by this study, this could be due to the pseudo-aliasing introduced by the lack of a topographic mass-density model, as well as distortions in the AHD.

Summary and Conclusions

This study has compared geoid models computed from mean Faye gravity anomalies (as approximations of Helmert gravity anomalies) derived from discrete gravity observations using two different gridding techniques. The first, termed the SB technique, grids simple Bouguer gravity anomalies, reconstructs free-air gravity anomalies using a DEM, then adds the mean terrain correction from all DEM elements within a 2' by 2' compartment to yield mean Faye gravity anomalies. The second, termed the RB technique, grids refined Bouguer anomalies, where the terrain corrections have been interpolated from the DEM grid to the discrete gravity observations, then reconstructs mean Faye gravity anomalies on the same 2' by 2' grid.

Two regional gravimetric geoid models were then constructed from these two grids of mean Faye gravity anomalies using the classical remove-compute-restore technique based on the complete expansion of the EGM96 global geopotential model, the entire rectangular gravity data area, and a spherical [unmodified] Stokes kernel. This was to deliberately accentuate the low-frequency differences between the resulting geoid models. The overall aim of this study was to determine if the theoretical possibility of pseudo-aliasing occurring when simple Bouguer gravity anomalies are gridded makes any significant difference in the Australian context.

The maximum difference between the computed geoid models reached only 14 cm, and is highly correlated with topography, notably along the eastern seaboard of Australia. Comparisons with 1013 Australia-wide GPS-levelling data showed that there was no significant difference between the two computed geoid models. Therefore, it can be concluded that, in Australia, the role of terrain corrections in reducing pseudo-aliasing during gravity gridding is insignificant given the current status and quality of the available data and the choice of data manipulation algorithms and data modelling techniques. Accordingly, the arguments presented by [**8**] in favour of the so-called SB technique appear to hold in the Australian context.

Acknowledgements

Firstly and mostly, we would like to thank Dr Dennis Milbert of the US National Geodetic Survey for prompting this investigation. We would also like to thank Geoscience Australia for providing the gravity terrain, GPS and levelling data, NASA and NIMA for providing EGM96, and Professor Cheinway Hwang, National University of Taiwan, for providing GMGA97. This research has been supported financially by: Curtin University of Technology; a travelling scholarship from Delft University of Technology; and Australian Research Council large grant A39938040 and discovery project grant DP0211827. Thanks are also extended to the reviewers for their time and effort taken to review this manuscript.

References

1. Andersen, O.B., P. Knudsen, S. Kenyon and R. Trimmer (1999) Recent improvements in the KMS global marine gravity field, *Bollettino di Geofisica Teorica ed Applicata*, **40**: 369-377.
2. Bracewell, R.N. (1986) *The Fourier Transform and its Applications (2nd ed)*, McGraw-Hill, New York, 474 pp.
3. Brigham, E.O. (1988) *The Fast Fourier Transform*, Prentice-Hall, London, 252 pp.
4. Carroll, D. and M.P. Morse (1996) A national digital elevation model for resource and environmental management, *Cartography*, **25**: 395-405.
5. Deng, X.L., W.E. Featherstone and C. Hwang (in press) Estimation of contamination of ERS-2 and Poseidon satellite radar altimetry close to the coasts of Australia, *Marine Geodesy*, **25**(4).
6. Featherstone, W.E. (1998) Do we need a gravimetric geoid or a model of the base of the Australian Height Datum to transform GPS heights?, *The Australian Surveyor,* **43**: 273-280.
7. Featherstone, W.E. (2002) Comparison of different satellite altimeter-derived gravity anomaly grids with ship-borne gravity data around Australia, *Proceedings of GG2002,* Thessaloniki, August [http://olimpia.topo.auth.gr/GG2002/contents.html]
8. Featherstone, W.E. and J.F. Kirby (2000) The reduction of aliasing in gravity observations using digital terrain data and its effect upon geoid computation, *Geophysical Journal International,* **141**: 204-212.
9. Featherstone, W.E. and W. Guo (2001) A spatial evaluation of the precision of AUSGeoid98 versus AUSGeoid93 using GPS and levelling data, *Geomatics Research Australasia*, **74**: 75-102.
10. Featherstone, W.E. and J.F. Kirby (2002) A new high-resolution grid of gravimetric terrain corrections for Australia, *Australian Journal of Earth Sciences*, **49**: 733-734.
11. Featherstone, W.E., A.H.W. Kearsley and J.R. Gilliland (1997) Data preparations for a new Australian gravimetric geoid, *The Australian Surveyor,* **42**: 33-44.
12. Featherstone, W.E., J.F. Kirby, A.H.W. Kearsley, J.R. Gilliland, G.M. Johnston, J. Steed, R. Forsberg, M.G. Sideris (2001) The AUSGeoid98 geoid model of Australia: data treatment, computations and comparisons with GPS-levelling data, *Journal of Geodesy*, **75**: 313-330.
13. Forsberg, R. and W.E. Featherstone (1998) Geoids and cap sizes, in: Forsberg R, Feissl M, Dietrich R (eds), *Geodesy on the Move*, Springer, Berlin, 194-200
14. Forsberg. R. (1998) The use of spectral techniques in gravity field modelling: trends and perspectives, *Physics and Chemistry of the Earth* **23**: 31-39
15. Fotopoulos, G., C. Kotsakis and M.G. Sideris, 1999, A new Canadian geoid model in support of levelling by GPS, *Geomatica*, **53**(4): 53-62.
16. Haagmans RRN, de Min E, van Gelderen M (1993) Fast evaluation of convolution integrals on the sphere using 1D-FFT, and a comparison with existing methods for Stokes's integral, *manuscripta geodaetica*, **18**: 227-241.
17. Heiskanen, W.H. and H. Moritz (1967) *Physical Geodesy*, Freeman, San Francisco, 364 pp.
18. Hutchinson, M. (ed) (2001) *User Guide for the GEODATA 9 SECOND Digital Elevation Model of Australia* (second edition), Australian Surveying and Land Information Group and Australian National University, Canberra. [http://www.auslig.gov.au/download/usrguide/9sdemv2userguide.pdf].
19. Hwang, C. (1998) Inverse Vening Meinesz formula and deflection-geoid formula: applications to the predictions of gravity and geoid over the South China Sea, *Journal of Geodesy*, **72**: 304-312,
20. Hwang, C., E-C. Kao and B.E. Parsons (1998) Global derivation of marine gravity anomalies from SEASAT, GEOSAT, ERS-1 and TOPEX/POSEIDON altimeter data, *Geophysical Journal International*, **134**: 449-459
21. Jekeli, C. (1996) Spherical harmonic analysis, aliasing, and filtering, Journal of Geodesy, **70**: 214-223

22. Johnston, G.M. and G.C. Luton (2001) GPS and the Australian Height Datum, *Proceedings of the 5th International Symposium on Satellite Navigation Technology and Applications*, Canberra, July [CD-ROM].
23. Kirby, J.F. and W.E. Featherstone (1999) Terrain correcting the Australian gravity database using the national digital elevation model and the fast Fourier transform, *Australian Journal of Earth Sciences*, **46**: 555-562.
24. Kirby, J.F. and Featherstone, W.E. (2001) Anomalously large gradients in the "GEODATA 9 SECOND" Digital Elevation Model of Australia, and their effects on gravimetric terrain corrections, *Cartography*, **30**: 1-10.
25. Kirby, J.F., W.E. Featherstone and A.H.W. Kearsley (1997) Geoid computations using ring integration: gridded versus point data, *Geomatics Research Australasia*, **67**: 33-46.
26. Lemoine, F.G., Kenyon, S.C., Factor, J.K., Trimmer, R.G., Pavlis, N.K., Chinn, D.S., Cox, C.M., Klosko, S.M., Luthcke, S.B., Torrence, M.H., Wang, Y.M., Williamson, R.G., Pavlis, E.C., Rapp, R.H. and Olson, T.R. (1998) The development of the joint NASA GSFC and the National Imagery and Mapping Agency (NIMA) geopotential model EGM96, *NASA/TP-1998-206861*, National Aeronautics and Space Administration, Maryland, USA, ~575 pp.
27. Murray, A.S. (1997) The Australian national gravity database, *AGSO Journal of Australian Geology and Geophysics*, **17**: 145-155.
28. Roelse, A., H.W. Granger and J.W. Graham (1971) The adjustment of the Australian levelling survey 1970-71, *Report 12*, Division of National Mapping, Canberra, Australia.
29. Sandwell, D.T. and W.H.F. Smith (1997) Marine gravity anomaly from Geosat and ERS 1 satellite altimetry, *Journal of Geophysical Research – Solid Earth*, **102**: 10039-10054
30. Schwarz, K.P., M.G. Sideris and R. Forsberg (1990) The use of FFT techniques in physical geodesy, *Geophysical Journal International*, **100**: 485-514.
31. Sideris, M.G. (1995) Fourier geoid determination with irregular data, *Journal of Geodesy*, **70**: 2-12
32. Smith, D.A. and D.G. Milbert (1999) The GEOID96 high-resolution geoid height model for the United States, *Journal of Geodesy* **73**: 219-236
33. Smith, W.H.F. and P. Wessel (1990) Gridding with continuous curvature splines in tension, *Geophysics* **55**: 293-305
34. Tziavos, I.N. (1996) Comparisons of spectral techniques for geoid computations over large regions, *Journal of Geodesy* **70**: 357-373
35. Tziavos, I.N. and W.E. Featherstone (2001) First results of using digital density data in gravimetric geoid computation in Australia, in: Sideris, M.G. (ed) *Gravity, Geoid and Geodynamics 2000*, Springer, Berlin, 335-340
36. Vaníček, P. and W.E. Featherstone (1998) Performance of three types of Stokes's kernel in the combined solution for the geoid, *Journal of Geodesy*, **72**: 684-697.
37. Vermeer, M. (1992) A frequency domain approach to optimal geophysical data gridding, *manuscripta geodaetica*, **17**: 141-154.
38. Wessel, P. and Smith, W.H.F. (1995) New version of the Generic Mapping Tools released, *EOS – Transactions of the American Geophysical Union*, **76**: 329.
39. Zhang, K.F. (1997) An evaluation of FFT geoid determination techniques and their application to Australian GPS heighting, *Ph.D. thesis*, School of Surveying and Land Information, Curtin University of Technology, Perth, Australia